Chapter 1
The Basis of Nuclear Magnetic Resonance Spectroscopy

Abstract Nuclear magnetic resonance (NMR) has transformed the research areas of Chemistry, Biochemistry and Medicine, but much of its fundamentals remain obscure for the non-initiated. NMR is a technique based on the absorption of radiofrequency radiation by atomic nuclei in the presence of an external magnetic field. In this chapter, we describe the physical basis of phenomena within NMR spectroscopy from both a quantum-theory perspective and a classical view, to provide any prospective user the basic concepts underlying the technique. The spectroscopic notion of energy level population is described, as well as a basic introduction to the theory and mechanisms of spin relaxation. The application of radiofrequency pulses to produce the NMR signal, its conversion to the frequency domain by Fourier Transform and the typical instrumental set-up of magnetic resonance are also covered.

Keywords Dipolar interaction · Gyromagnetic · Magnet · Nuclear magnetic resonance (NMR) · Nuclear spin · Quantum levels · Radiofrequency pulse · Relaxation · Spectroscopy

1.1 Introduction

The aim of this chapter is to give a brief summary of the physical basis of nuclear magnetic resonance (NMR) spectroscopy. The theoretical description provided here is not exhaustive, and the interested reader is encouraged to refer to more advanced texts for further information (Ernst et al. 1987; Günther 1995; Wüthrich 1986; Derome 1987; Claridge 1999; Cavanagh et al. 1996; Keeler 2006; Evans 1996; Sanders and Hunter 1992). In our treatment of NMR theory, we shall introduce the classical vector approach and a naïve quantum mechanical approach, trying to avoid, for the sake of simplicity, the complicated mathematics behind the theory.

R. J. Carbajo and J. L. Neira, *NMR for Chemists and Biologists*,
SpringerBriefs in Biochemistry and Molecular Biology,
DOI: 10.1007/978-94-007-6976-2_1, © The Author(s) 2013

NMR is based on the magnetic properties of atomic nuclei, which may be considered to be composed of spinning particles in the simplest model. NMR uses an effect which is well-known in classical physics: when two pendulums are joined by a flexible axle and one of them is forced into oscillation, the other is forced into movement by the common flexible support and the energy will flow between the two. This flow of energy is most efficient when the frequencies of the two movements are identical: the so-called *resonance* condition. Another example of the resonance condition is found in radio antennas. A radio antenna responds to broadcast radiofrequency signal through the movement of electrons, which shift up and down in the antenna at the same frequency as that of the broadcast signal. In both examples, resonance (the same frequency) is the key, as it is in NMR. In NMR, instead of electrons or pendulums, there are nuclear spins; therefore, we need first to understand how electromagnetic radiation interacts with those spins.

1.2 Physical Principles of NMR Spectroscopy

1.2.1 The Basis of NMR Spectroscopy: A Vector Approach

For an introduction to the classical formalism in NMR, the interested reader can have a look in the literature (Farrar and Becker 1971). From a classical physical perspective, a charge travelling circularly around an axis builds up a magnetic moment (dipolar moment or magnetic dipole), μ, with a direction perpendicular to the plane defined by the circular movement of the charged particle. The faster the charge travels, the more intense the induced magnetic field and the stronger the magnetic dipole. Atomic nuclei contain positively charged particles which have such rotating movement and consequently generate nuclear magnetic dipoles. In the presence of an external static magnetic field, B_0, the magnetic moment μ of the nuclear particles will orient either with (parallel) or against (anti-parallel) B_0. This interaction causes a movement of precession of the nuclear dipoles around the B_0 axis (Fig. 1.1a), in a manner analogous to a gyroscope in a gravitational field; this precession is a consequence of the rotation about the own nuclear axis of the particle. The angular frequency of this precession, ω, depends on: (i) the strength of B_0; and (ii) the properties of each particular nucleus. This frequency is called the *Larmor frequency* and is given by $\omega = 2\pi\upsilon = \gamma B_0$, where the proportionality constant γ is called the *gyromagnetic* or *magnetogyric* ratio and υ is the *frequency*. It is important to emphasise that the precession is only possible in the presence of an external B_0.

The Boltzmann distribution dictates that the most stable and lowest energy state in a system will be the most populated at equilibrium. In this case, the nuclear magnetic dipoles oriented with B_0 have the lowest energy. However, the difference in energy with the less stable state (dipoles oriented against B_0) is small, leading to a small difference in population. Although minor, the population imbalance leads to a net nuclear magnetic moment, which is the sum of the dipole moments

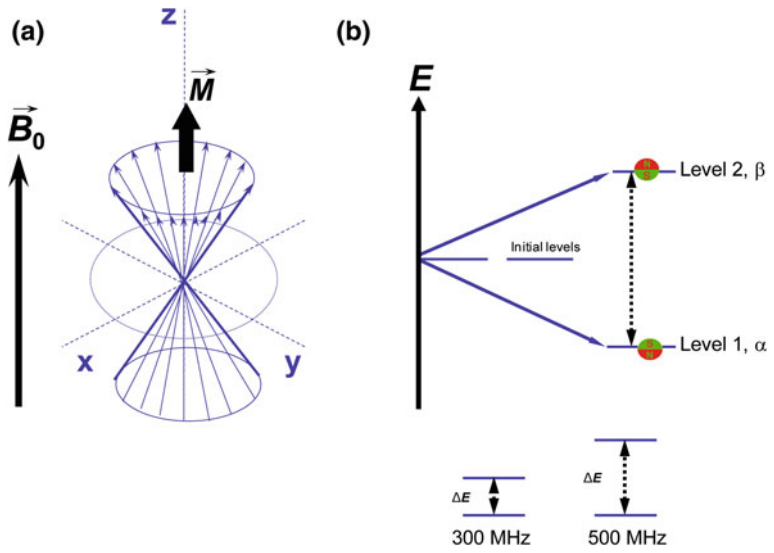

Fig. 1.1 The physical basis of NMR. **a** Classical view of NMR. Spins precess around the external magnetic field B_0; the net magnetization of the system (the sum of all the nuclear magnetic dipoles of the sample) is shown along the z-axis as *M*. The *thin arrows* are the magnetic dipoles of each nucleus. **b** Quantum view of NMR. The two quantum levels originated as a consequence of B_0 (*left* side) are shown (for the sake of simplicity, it has been assumed that the nuclear spin has only two possible orientations, as for the ^{1}H atom); the orientation of the two spins is indicated as small circles in each level showing the polarity of the nuclear magnets. The *dotted arrow* indicates the jump from one quantum level to the other. The arrow on the *left* side of the figure represents the energy. To allow for a comparison, at the *bottom* of the figure two split levels are shown for a 300 and 500 MHz magnets (the figure is not to scale)

(vectors) of all nuclei present in the sample. This net nuclear magnetic moment is called *magnetization* (*M*), and it is represented by a vector parallel to the static magnetic field B_0 (Fig. 1.1a). The length of the *M* vector is proportional to the population difference between the parallel and antiparallel dipolar moments. If an appropriate amount of energy is applied, *M* will move from its equilibrium position to become oriented with B_0 (–*M*). The corresponding absorption of energy experienced by the nuclei in that action is measured by NMR and the energy is in the order of that of radio waves.

1.2.2 The Basis of NMR Spectroscopy: A Naïve Quantum Approach

From the perspective of quantum mechanics, the magnetic resonance phenomenon takes place due to an intrinsic property of nuclei: the *spin* (the rotation around its own nuclear axis). To introduce spin we shall consider a simple particle like the

Table 1.1 Predicting the nuclear spin (*I*)

Number of protons (Z)	Number of neutrons	Nuclear spin (*I*)
Even[a]	Even	0
Even	Odd	1/2, 3/2,…
Odd	Even	1/2, 3/2,…
Odd	Odd	1, 2,…

[a] 0 is considered here an even number

familiar electron. The electron has spin, which is the source of its angular momentum (due to its rotation movement), taking a value of ½. Since in quantum mechanics each moment l has $2l + 1$ associated values, the value of ½ means that there are $(2 \times ½) + 1$ different possible levels, with quantum numbers ½ and –½. In the absence of an external magnetic field, both levels have the same energy (they are degenerate). In the presence of an external magnetic field, the two levels become separated by a difference in energy ΔE.

Similarly to the electron, atomic nuclei have *spin angular momentum*, represented by I. The value of I for each nucleus depends on its atomic structure (number of protons and neutrons) (Table 1.1). As a consequence of the spin, the nucleus has an associated *dipole moment* (μ), which takes the value $\mu = \gamma I$. Analogous to the electron spin angular momentum, the nuclear spin angular momentum is quantized and can only take $(2I + 1)$ discrete values, given by the quantum number m_I. These discrete values are energetically degenerate (as with the electron levels) in the absence of any external magnetic field, but in the presence of B_0, quantized (discrete) energy will separate the two levels. For instance, a proton (^{1}H) has $I = ½$ (like the electron) and its spin can adopt either of two orientations (½ or –½), which are degenerate in the absence of an external field (B_0). The state with $m_I = ½$ (↑), known as α, is oriented parallel to the external B_0, whereas that with $m_I = -½$ (↓) and denoted by β, represents the antiparallel orientation to the external B_0 (Fig. 1.1b). For those nuclei with spin ½ and $\gamma > 0$, the α state has a lower energy than the β state. On the other hand, nuclei with $I = 1$, like ^{14}N, will show three energy levels, in the presence of B_0, corresponding with m_I taking the values 1, 0, –1. Nuclei with $I = 0$ (such as ^{12}C) do not have dipole moment μ, no energy levels to be split and therefore no NMR signal.

The energy difference between the levels is determined by $\Delta E = \mu B_0$, and presents values within the radiofrequency spectrum. Therefore, the larger B_0, the larger the energetic separation and the resulting population differences (Fig. 1.1b, bottom). With currently available magnets the energy gap is quite small (at room temperature, for an 11.1 T magnet the difference between the populations for protons is in the order of 1 in 10^{-5}) which is the basis for the inherent low sensitivity of NMR spectroscopy. To induce a transition between the energy levels, it is necessary to apply an electromagnetic radiation with an amount of energy given by the Planck equation. Absorption of applied radiation, that satisfies the resonance condition (of the Larmor frequency), causes a spin-½ nucleus to flip from the α (low energy) to the β (high energy) state. These changes in energy

levels are referred as *NMR transitions*. A net absorption of energy is possible as long as the population of nuclear spins in the higher energy level is smaller than in the lower one. When, in the presence of an applied B_0, the populations of the two levels become equal, the system is saturated and no further absorption of energy will ensue. We shall discuss later (Sect. 1.3) how a system can return to the equilibrium state, where the lower energy level is more populated.

1.2.3 The Nuclei in NMR

If the number of both the protons and neutrons in a given nuclide are even, such as in the most abundant isotope of carbon ${}^{12}_{6}C$, then $I = 0$ and thus, there can be no NMR signal (Table 1.1). On the other hand, those nuclei with an odd number of either protons or neutrons will have a half-integer spin (i.e. ½) and those presenting an odd number for both protons and neutrons will have a spin >½ (e.g. 1, 3/2, 5/2, etc.). The number of neutrons varies within each chemical element giving rise to its isotopes, thus for each individual element there might be one or more NMR-active isotopes. Among the ½ spin nuclei, the most interesting nuclides are ^{1}H and ^{13}C because of the ubiquity of these elements in the structure of natural molecules. The ^{15}N, ^{19}F or ^{31}P (Table 1.2) nuclei are also much used and chemically interesting although any isotope with $I \neq 0$ can in principle be detected by NMR. A comprehensive description of the NMR properties of all the nuclei in the periodic table can be found in the literature (Harris and Mann 1978; Mason 1987). It is important to note that the value of γ is different among the nuclei. Since the separation among the levels in the presence of an external magnetic field (Fig. 1.1b) relies on γ, it is clear that the larger a nuclide's γ value, the larger the separation between levels, and therefore the better its sensitivity in NMR experiments.

Table 1.2 Magnetic properties of selected nuclei

Isotope	I	γ 10^7 (T^{-1} s^{-1})[a]	Abundance (%)
^{1}H	1/2	26.75	99.985
^{2}H	1	4.11 (2.8 10^{-3})	0.015
^{14}N	1	1.93 (1.0 10^{-3})	99.63
^{15}N	1/2	−2.71	0.37
^{12}C	0		98.89
^{13}C	1/2	6.73	1.108
^{16}O	0		99.96
^{17}O	5/2	−3.627 (−2.6 10^{-2})	0.037
^{19}F	1/2	25.18	100.0
^{31}P	1/2	10.83	100.0
^{33}S	3/2	2.05 (−5.5 10^{-2})	0.76

[a] Quadrupolar moment indicated in 10^{-28} m^2 (for nuclei with $I > 1/2$)

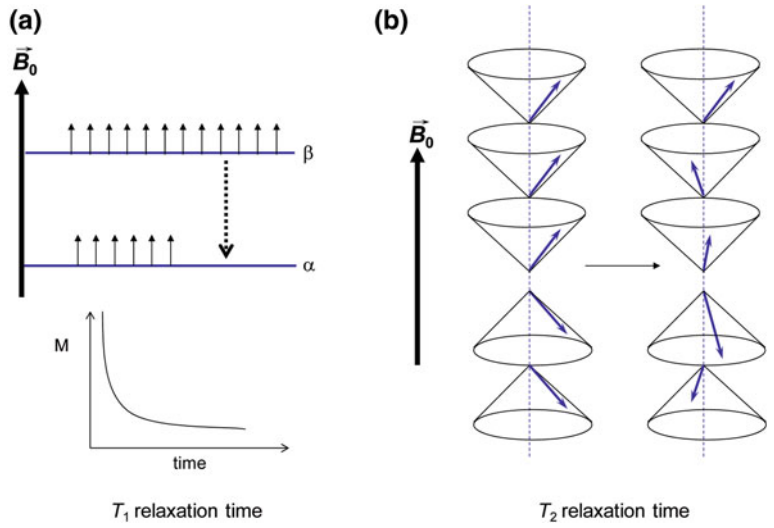

Fig. 1.2 Spin relaxation. **a** The longitudinal spin–lattice relaxation time (T_1) is the time constant for the exponential return of the magnetization to the equilibrium population. The arrows represent the population of spins. The graphics at the *bottom* represent the exponential behaviour that the recovery of the equilibrium population (represented by M) follows (indicated by the *thick dotted arrow* in the *upper* panel). **b** The transversal spin–spin relaxation time (T_2) is the time constant for the exponential return of the spins to a random distribution of their phases (the angle formed between the precessing spins and the external field B_0). No change in population is observed in this type of relaxation, and therefore no energy is transmitted from the spins to their neighbourhood

Nuclei with $I > ½$ (Table 1.2) display two characteristic features. First, they will show $(2I + 1)$ quantum states which lead to more complicated transitions than the single jump between the two levels of a spin-½ nucleus. Second, they show an asymmetric distribution of charge leading to a nuclear electric quadrupole, which gives them the common name of *quadrupolar* nuclei. An electric quadrupole can be visualized as a charge distribution similar to the four lobes of an atomic *d*-orbital (in this analogy, an electric dipole would correspond to a *p*-orbital), which is a non-spherical charge distribution. Such arrangement results in a strong interaction with the electric field gradients generated by the non-uniform distribution of local electronic charges at the nucleus. Moreover, the quadrupole is coupled to the nuclear μ that is also present in these nuclei. All these effects lead to quadrupolar relaxation effects that are responsible for the broadening and poor resolution of their NMR signals (Sect. 1.3). This broadening, together with their often reduced sensitivity (small γ) or low natural abundance, are the main reasons for the relatively low popularity of the NMR investigation on quadrupolar nuclei.

1.3 Spin Relaxation

In this section, we describe how the populations of spins recover after the excitation and return to their equilibrium distribution. Importantly, these so-called *relaxation mechanisms* can also provide information on the dynamics of the molecules. For clarity purposes, we shall restrict the discussion to a spin-½ nucleus.

In the equilibrium state, the system only possesses longitudinal magnetization (along the z-axis: the M vector in Fig. 1.1a), and not a transverse one (that is, in the xy-plane). From a quantum perspective, apart from the uneven populations in the two quantum levels, this means that the individual spins, at equilibrium, have a random distribution of phases of their wave-functions (the states α or β of the particular spin). After the absorption of energy two steps are needed for the return to equilibrium: the restoration of the initial populations (that is, M aligned with the z-axis) and the randomization of the phases of the wave-functions of the nuclear spins. In NMR, the absorption of energy is produced by an externally oscillating electromagnetic field (that is, a radiofrequency; Sect. 1.4), and relaxation is also induced by oscillating magnetic fields within the molecules (for example, other spins in the same or different molecules within the sample). Hence, relaxation in NMR occurs by magnetic interactions. This variation in the internal oscillating magnetic fields is modulated by molecular motion and it is a property of the local environment of each particular spin.

At this stage, it is important to recognize the difference between the relaxation processes in NMR and other spectroscopies, where the recuperation of the equilibrium population occurs by collisions with other molecules and dissipation of energy by heat release. The collision is extremely slow and inefficient in NMR, as collisions involve mainly the electronic shells of the nuclei. This leads to NMR excited states with lifetimes in the range of milliseconds to seconds compared to excited molecular states with lifetimes as short as μs to ns in other spectroscopic techniques. This extended lifetime of excited states is crucial to the success of NMR, since it does not only mean that the signals are narrower than in other spectroscopies (according to the Heisenberg uncertainty principle), but also allows the manipulation of the spins after the excitation, leading to the myriad of different experiments available which result in the richness of the technique and its applications.

1.3.1 Spin–Lattice Relaxation Time

We have already described how for our spin-½ nucleus in the presence of an external field, B_0, two quantum levels α and β will separate. Electromagnetic radiation with the adequate υ will cause transitions to occur between those two levels, with spins jumping from the lower to the higher one. If the resonant absorption continues, it seems evident that after a certain time the number of spins

at the β level will match that in the α state. When the two populations become equal, the intensity of the NMR signal decreases because a "saturated" state has been reached. The situation is similar to that experienced by youngsters (the spins), trying to enter into a popular disco (the upper level) where a delicious drink/beat/music… (the energy) is provided; if the disco is full (saturation) no net entry of people (the intensity) within the venue can take place.

Non-radiate processes (those which do not cause emission of electromagnetic radiation, but rather emission of heat) by which β nuclear spins can become α spins again occur. Interactions between the spins and their surroundings, also known as the *lattice*, lead to loss of energy. These non-radiate processes, by which the population of nuclear spins returns to equilibrium (in the classical model, magnetization recovering its *longitudinal* position parallel to B_0), follow an exponential behaviour, dependent on the *spin–lattice* relaxation time (or longitudinal time), represented by T_1 (Fig. 1.2a). It is important to emphasise that T_1 describes the time taken by the magnetization to recover the position aligned with the z-axis, and during that time the population of the system reverts to the uneven distribution of the equilibrium populations. Finally, it is important to bear in mind that some authors describe the spin–lattice relaxation rate ($R_1 = 1/T_1$) instead of a spin–lattice relaxation time T_1 (Sanders and Hunter 1992).

1.3.2 Spin–Spin Relaxation Time

We shall continue to consider a spin-½ system, this time with three spins precessing aligned along B_0 and two precessing against B_0 (note that we are not saying that this situation corresponds to the equilibrium population) (Fig. 1.2b, left). If each spin has a somewhat different Larmor frequency (due, for instance, to a dissimilar chemical environment or to field inhomogeneity), they will gradually fan out and, at thermal equilibrium, the entire set of vectors will lie at random angles to the direction of the B_0 (Fig. 1.2b, right). It is important to point out that the population of the two spin-states has not been altered, and that there is no transfer of energy to the surroundings in this case, as described in spin–lattice relaxation. The time governing this exponential behaviour, which returns the system to a random arrangement of phases, is called the *spin–spin* (*transversal*) relaxation time T_2 (the second factor mentioned above when we were describing how to restore the equilibrium population). In some texts, the spin–spin time is again represented as the relaxation rate $R_2 = 1/T_2$ (Sanders and Hunter 1992). We shall return to the meaning of *transverse* for T_2 later when we describe the effect of pulses on magnetization (Sect. 1.4).

Taken together, we can say T_1 acts as the enthalpic component to restore the equilibrium population (since there is a rearrangement of the populations), and T_2 works as the entropic component in the restoration of the equilibrium (since it involves disorder of the phases of the spins).

1.3.3 Sources of Variation in Local Fields

Variation in the local magnetic field is one of the factors responsible for the relaxation mechanisms, but what causes these? In this section we shall describe the sources of the local fields, whose variations cause both spin–lattice and spin–spin relaxation processes. The key point in the discussion is that local fields fluctuate both in magnitude and direction, depending on the orientation and movement of the molecule with respect to the applied B_0.

1.3.3.1 Dipole–Dipole Interactions

The mechanism of nuclear spin relaxation lies predominantly in magnetic interactions, of which the most important one is *dipole–dipole* relaxation or *dipolar* interaction, in short. This type of interaction is also the source of the *nuclear Overhauser enhancement* or NOE effect (Chap. 2). Dipolar interactions can be easily grasped using the classical view of nuclei as bar magnets. The dipolar coupling between two magnets depends on the distance between them, as well as on the external B_0 (Fig. 1.3a). If we replace these two magnets by the spins of two nuclei, A and B, within a molecule that tumbles randomly in solution, this random movement will alter the internuclear vector r_{AB}. Additionally, the local field experienced by any nucleus will fluctuate randomly as the result of variations in its surroundings. Random motion of a molecule occurs due to molecular collisions, and can be characterized by the *correlation time*, τ_c, which is usually defined as the average time it takes a molecule to rotate one radian ($\sim 57°$). Long τ_c times correspond to slow tumbling of the nuclei (as found for macromolecules), and short τ_cs correspond to fast tumbling (as displayed by small molecules).

Which kind of local magnetic fields can induce a transition from β to α (that is, spin–lattice relaxation)? The ideal field would be one that fluctuates at a frequency close to the Larmor frequency of the involved nuclei. Such field can arise from the tumbling motion of the molecule. If the frequency of this molecular tumbling is slow compared to the Larmor frequency, it will cause an oscillating magnetic field that fluctuates too slowly to induce transitions and consequently T_1 will be long. Conversely, if the frequency of the molecular tumbling is faster than the Larmor frequency, this fluctuating field will oscillate too fast to induce transitions, and therefore T_1 will be long again. Only when the frequency of the tumbling rate is about the same as the Larmor frequency, T_1 will be short, and the molecule will show fast relaxation. It is important to bear in mind that the rate of molecular tumbling increases with temperature and with the decrease of the viscosity of the solvent (Fig. 1.3b).

What are the most effective local dipolar interactions to induce spin–spin relaxation? The most favourable ones would be those presenting an interaction at a relatively slow variation rate. Under the influence of this slowly-changing local magnetic field, each nuclear spin in the sample remains in its local magnetic

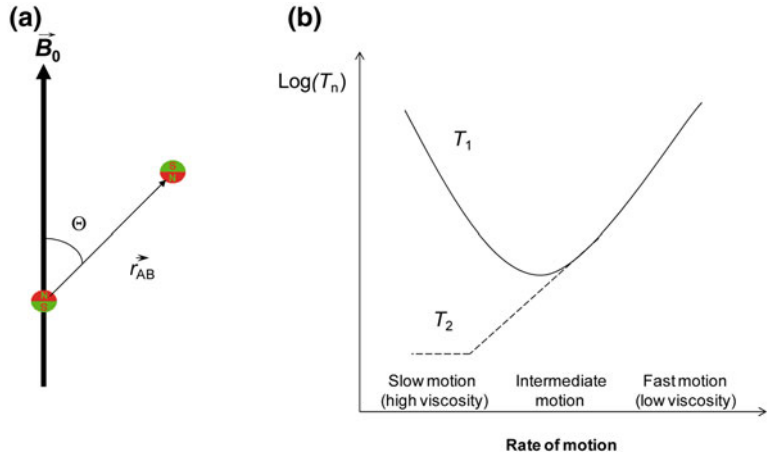

Fig. 1.3 Variations in the local fields. **a** Physical parameters on which the dipolar–dipolar interaction relies: the distance between spins r_{AB}, and the angle Θ formed between the r_{AB} vector and the external magnetic field B_0. **b** Variation of the longitudinal and transversal relaxation times with the molecular movement rate (either by tumbling or migration through the solution), which depends, in turn, on changes of temperature or viscosity

environment, giving the spins enough time to randomize their orientations. Obviously, this will preferentially occur at low temperatures, in high viscosity conditions, or in very rigid molecules (e.g. solid-state samples). Conversely, if the molecule moves very fast (for instance, at high temperature or low viscosity) T_2 increases and the randomization does not take place. That is, slow molecular motion corresponds to short T_2 times, and fast molecular motion corresponds to long T_2s. T_2 is always smaller than T_1, but at high temperatures both relaxation times become close to equal (Fig. 1.3b).

For nuclei relaxing mainly through dipolar interactions, the line-width of the signals in the spectrum is determined by: (i) the proximity of other nuclei; and (ii) the value of τ_c. For instance, the line-width of the signals in the NMR spectra of large biomolecules is very broad due to their associated slow overall tumbling. The relaxation via dipolar interactions can also arise from the magnetic interaction of a nuclear spin with an unpaired electron, which also behaves as a miniature magnet. This effect is known as *paramagnetic relaxation*. As the magnetic moment of an electron is over 1000 times that of a proton, this relaxation mechanism is very efficient; in fact, this dipolar interaction is used to deliberately reduce the relaxation times of spins in molecules with a high number of isolated nuclei by adding agents containing paramagnetic species, such as derivative of metals of the series d and f of the periodic table (e.g. Cr(III) in $Cr(acac)_3$).

1.3.3.2 Chemical Shift Anisotropy

The local variation of fields is a direct result of the anisotropic electronic environment of molecules, which "shields" or "unshields" nuclei from the external magnetic field in an orientation dependent manner. This varying field can stimulate relaxation if it is sufficiently strong. Chemical Shift Anisotropy (CSA) is important, for instance, in atoms having sp^2 hybridization and therefore non-spherical electronic charge distribution. The CSA contribution to spin relaxation correlates quadratically with B_0 (that is, CSA becomes more significant at higher fields), but is usually less relevant than dipolar interactions. In biomolecules, ^{13}C, ^{15}N and ^{31}P nuclei have significant CSA contributions.

1.3.3.3 Quadrupolar Relaxation

In low-symmetry environments quadrupolar nuclei ($I > ½$; Sect. 1.2.3) experience non-zero electric field gradients, which depend on the molecular orientation with respect to B_0. This anisotropic interaction is modulated as the molecule tumbles at an appropriate frequency (as in the dipolar interactions), inducing flipping of nuclear spin states, and therefore, spin relaxation. Relaxation of quadrupolar nuclei is governed by the features of the quadrupole nucleus itself and the electric field gradient, which depends on the local environment. Therefore this relaxation mechanism is electric-dependent rather than magnetic. In general, the larger the quadrupole and the electric field gradient, the more efficient the relaxation mechanism is, due to shorter T_2s. On the other hand, quadrupolar nuclei in highly symmetrical environments (tetrahedral or octahedral structures) have electric field gradients close to zero, and the quadrupolar relaxation mechanism is ineffectual. For instance, the NMR spectrum of ^{14}N ($I = 1$) in tetrahedral NH_4^+ has a line-width in the range of 1 Hz, but pyramidal NH_3 (a less symmetrical environment than a tetrahedron) has line-widths close to 100 Hz.

1.3.3.4 Spin-Rotation Relaxation

Small molecules, or groups of atoms in a large molecule (e.g. methyl groups), can rotate rapidly in low-viscosity solvents, thus creating a molecular magnetic moment due to the rotating electronic and nuclear charges. The local field associated with this magnetic moment is modulated by molecular collisions and movements, providing another nuclear spin relaxation mechanism: the so-called *spin-rotation* relaxation. This mechanism is more effective in small, symmetrical molecules or freely rotating groups, and the relaxation efficiency increases with the reduction of rotational correlation times.

1.3.3.5 Scalar Relaxation

Relaxation may also be induced when a nucleus is scalarly coupled (Chap. 2) to another one which fluctuates rapidly. This fluctuation might originate from: (i) chemical exchange of the coupled nucleus; or (ii) fast T_1 of the fluctuating nucleus (common in quadrupolar nuclei). A practical example is observed for nitrile groups (–C≡N), where the carbon is covalently bound to the quadrupolar ^{14}N nucleus resulting in a significant broadening of the ^{13}C signal.

1.4 Pulse Techniques

In most spectroscopic techniques such as UV or IR, experimentalists obtain spectra by varying the wavelength of the excitation source. A similar approach can be taken in NMR: varying the wavelength of the radiofrequency source will sequentially induce transitions of different atomic nuclei between their quantum levels (Fig. 1.1b). Alternatively, the same effect can be accomplished by keeping the excitation radiofrequency constant while varying the external field. For technical reasons, the latter approach is more practical in NMR and it is applied extensively.

In the early times of NMR (in the fifties to seventies of the last century), NMR magnets applied the slow-passage *continuous-wave* (CW) method, which involved the variation of the external B_0 to reach the resonance condition (the name comes from the continuous application of one radiofrequency while resonance is observed). Modern pulse methods excite the entire radiofrequency region of the nucleus of interest by applying a single variation of radiofrequency power (a pulse) and the resulting signals are recorded after the radiofrequency is turned off. A Fourier transformation (FT) is required to convert the resulting signal into the familiar NMR spectrum and, therefore, pulse-NMR is often called FT-NMR. One of the best analogies for comparing the old and new ways to acquire NMR spectra is the detection of the spectrum of sounds (vibrations) of a bell-ladder (a set of nearby bells with different sizes, joined by their closed termini). If we sequentially strike each of the bells with a unique hammer, we will collect the single sound (frequency) of a particular bell. Conversely, if we strike the whole set of bells forming the ladder, we shall produce a clang contributed by all the frequencies of each particular bell. Our challenging mission will be to disentangle the particular frequencies within that clang. In NMR, the "bells" are our nuclear spins, and the "clang" of frequencies is the magnetization decay of the spins as they return to equilibrium after excitation with a radiofrequency pulse (the "hammer").

1.4.1 How a Pulse Works: The Time and Frequency Domains

In this section, we describe first how the pulse affects the magnetization (M) of a system in the presence of B_0, and how we obtain the time and frequency domains of an NMR spectrum.

1.4.1.1 The Effect of a Radiofrequency Pulse: Changing the Observation System

Since most of the tiny magnetic dipoles within the atoms–but not all, due to the Boltzmann distribution at equilibrium–are aligned with the external field, there is a net magnetization M along the direction defined by B_0 (in the classical view). If we apply a short (in the order of microseconds) radiofrequency perturbation (a *pulse* or the so-called B_1) along the x-axis (Fig. 1.4a), with a frequency matching the separation energy between the quantum levels (or, in other words, the Larmor frequency in the classical view), the spins aligned initially with the z-axis will move away from that axis and onto the xy-plane.

The B_0 is larger than the B_1 field by many orders of magnitude. For instance, in the case of the ^{1}H nucleus the B_0 field corresponds to precession frequencies of hundreds of MHz, whereas the B_1 is about 1–20 kHz. The B_1 field is not static, but it rather rotates about the z-axis (the axis of the B_0) with a frequency that closely matches the Larmor frequency of the spins that originate from M. Under the influence of these two magnetic fields, M will start precessing around B_1 (with a frequency $\omega = \gamma B_1$) simultaneously as it does around B_0 (with $\omega_0 = \gamma B_0$), in a motion called *nutation*. In order to pave the way for a better understanding of the effect of B_1, we need to change our system of reference. Before, we have been observing the precession of the spins around B_0 from our "laboratory system" (the so-called "frame system"; that is, the system from where we have applied the B_0). If we change our observation system to one that rotates at the Larmor frequency, ω_0, we shall not notice the rotation of the spins, in the same way we do not feel the rotation of the Earth around its axis, because we are within the "Earth-observation system". In this *rotating frame of reference*, those spins whose Larmor frequency is exactly ω_0 will experience a null effective field, only feeling the effect of B_1 while precessing about its axis as long as B_1 is turned on. Spins with a slightly different precession frequency than the Larmor one will experience a precession around an effective magnetic field resulting from the sum of the "felt" B_0 and the applied B_1 (Fig. 1.4b).

Since B_1 is only applied for a short period of time, the effect on M is only a partial revolution around the B_1 axis, with the result of M being "tipped" towards the y-axis. The tip angle α (in radians) is given by $\alpha = \gamma B_1 t_p$, where t_p is the duration of the radiofrequency pulse (this expression is easily obtained from the equation of a uniform rotational movement: $\omega = \alpha/t_p$, and then $\alpha = \omega\, t_p = \gamma B_1 t_p$).

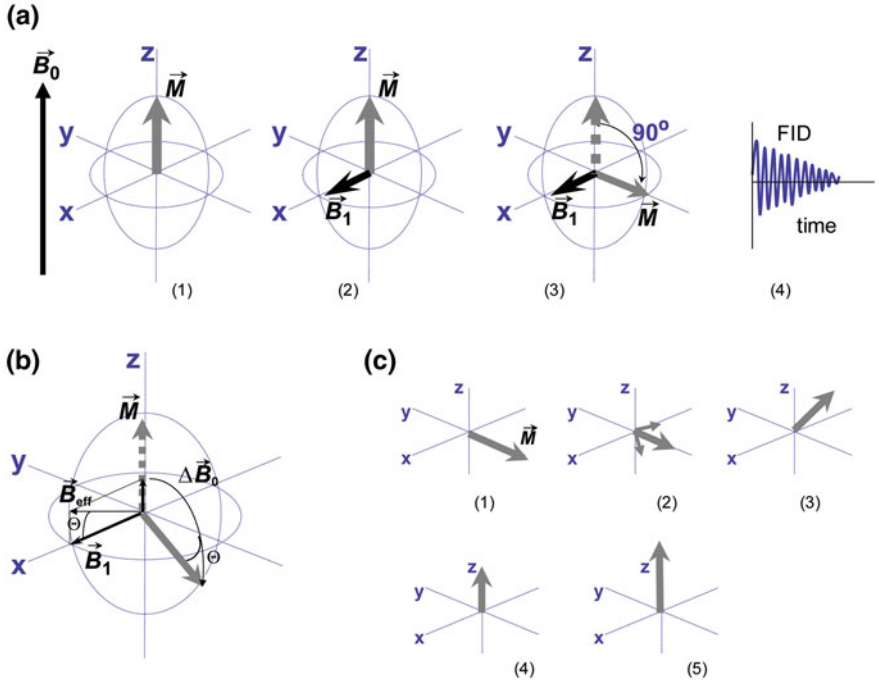

Fig. 1.4 Pulses in NMR. **a** How does a pulse work? Starting from the system at equilibrium (1) in the presence of an external magnetic field B_0 (left-hand side), a $(90)_x$-pulse (shown as B_1) is applied along the x-axis (2), with the effect of tilting the magnetization M (grey arrow) away from the z-axis and onto the xy-plane (3). This tilted magnetization evolves with time to recover its equilibrium position, and this decay renders the FID (4). **b** Scheme of the resulting field "felt" by spins whose precession frequency does not match the Larmor frequency of the "rotating frame" (the so-called *off-resonance* spins). In these spins, a component of B_0 (ΔB_0, the off-resonance value) adds to the pulse (B_1); the resulting "effective" field (the addition of ΔB_0 and B_1) is B_{eff}, which forms an angle Θ with the x-axis; this B_{eff} leaves the spins out of the y-axis, and therefore out of the xy-plane after a $(90)_x$-pulse has been applied. **c** Behaviour of M (*grey arrow*) after the application of a $(90)_x$-pulse within the "rotating frame of reference": (1) immediately after the $(90)_x$-pulse; (2) field inhomogenities appear (for reader's sake only two isochromatic spins are shown here) giving rise to T_2-effects; (3) T_1 relaxation tilts M back to the z-axis; (4) due to T_2-effects, when M returns to the equilibrium position along the z-axis, the phases of the spins are different (that is, a complete loss of magnetization in the xy-plane has occurred) and M has not recovered the full original length at equilibrium; (5) complete restoration of the equilibrium M occurs after sufficient time is allowed

The pulse is described according to: (i) the tilting it produces in M; and (ii) the axis on which it is applied. For instance, the term $(\pi/2)_x$ or 90_x indicates a pulse directed along the x-axis, which results in a 90° tilting (or $\pi/2$ radians) on the y-axis. The time length of a 90_x pulse for ^{1}H in a 500 MHz spectrometer is around 5–10 μs, with a field B_1 of 10^{-4} T, compared to the B_1 field of 10^{-8} T used in CW spectrometers. It is important to note that when the pulse is applied all spins

experience the same effect, generating what some authors call *coherences* (in the quantum view, the phases of all the wave-functions of the excited spins are the same) (Günther 1995; Wüthrich 1986; Derome 1987; Claridge 1999; Cavanagh et al. 1996; Keeler 2006; Evans 1996) (Sect. 1.3).

We can further elaborate on the meaning of t_p in the above expression by using the Heisenberg uncertainty principle (energy-time). This principle states that there is a minimum uncertainty (given by the Planck constant) in the simultaneous specification of both the energy of a system (and hence, the range of frequencies excited in the NMR) and the duration of the measurement (that is, t_p). If t_p is very short, then the range of frequencies excited is very large (i.e. there is a large uncertainty in the range of frequencies excited); this is commonly called a "hard" pulse. On the other hand, if t_p is very long (a so-called "soft" pulse), then the range of frequencies excited is very small (its uncertainty is very small) and we have a small range of nuclei (large selectivity) being excited. This soft pulse can be used to selectively excite some frequencies in the spectrum while leaving the rest unaffected. A common application consists in the selective saturation of the water signal in biomolecular samples, where the soft pulse is applied in a continuous way.

1.4.1.2 The Time Domain

For nuclei whose Larmor frequencies match exactly the frequency of the rotating frame of reference, once the perturbation on the spins in the form of the pulse is removed, the tilted M will stay forever on the y-axis in the absence of relaxation effects. However, with time the different spins forming the net M will start to disperse with their different precession frequencies, returning to the z-axis due to T_1-relaxation effects. On top of this, the inhomogeneities in B_0 cause different regions of the sample to "feel" slightly different B_0 fields, and therefore different Larmor frequencies (which is related to T_2). Thus, the projection of M on the y-axis will shrink according to T_1- and T_2-relaxation times (Sect. 1.3) leading to an exponentially decreasing signal termed the *free induction decay* (or in short, FID). The FID is named for the fact that the collected signal is "free" of the influence of B_1, it is "induced" in the coil and "decays" back to equilibrium. When M is on the y-axis and the magnetization starts to relax its way back to the z-axis due to T_1, the projection of M on the xy-plane will start decreasing as well as fanning out in the plane. The rates of both processes (decrease and fanning) depend on T_2 and hence the name of *transverse* as opposed to *longitudinal* relaxation, which occurs along the z-axis. In modern NMR instruments the setup of the receiver coil is usually along the x or y-axis (Sect. 1.5.4), and the FID is therefore directly related to T_2. The mathematical expression $\exp(-t/T_2)$ defines the envelope of the FID giving the maximum value possible for the transversal magnetization: the exponential decrease of the y-axis magnetization component of M will induce the change in the voltage of the receiver coil, allowing the recording of the FID. However, it is observed in all cases that the FID decays much more rapidly than

the value obtained from that envelope. This faster decay is due to real magnet inhomogeneity, which is, in turn, the principal source of T_2-relaxation effects.

Since (i) the effects of both relaxation times (decreasing the projection of the M vector along the x and y-axis (T_2-relaxation) and increasing the projection of the magnetization vector along the z-axis (T_1-relaxation)) add together; and (ii) T_2-relaxation time is shorter than T_1 (and therefore, the y-axis component of M decays to zero before the Boltzmann distribution is recovered) we shall have in the end an intermediate position (Fig. 1.4c) where M is on the z-axis, but its full equilibrium value is not completely recovered. However, after some extra time M will fully return to its equilibrium value with its vector length completely recovered.

It is important to remark that each point in the FID contains information about every resonance that will be observed in the final spectrum (see below). The more data we collect and the longer the period we observe the signal, the higher the resulting spectral resolution. However, if for any reason the signal decays too fast (because of a short T_2) we will not be able to record more useful information in the FID regardless of how long we keep collecting data. The FID is equivalent in our bell analogy above to the "clang" emitted by the bell-ladder, but instead of having all the frequency information as a sound, it is time-encoded, the so-called *time-domain*. Traditionally, the FID is recorded for a specific t_2 time (note that this is an "observation" time, different to the relaxation time T_2) (Fig. 1.4a, right).

1.4.1.3 The Frequency Domain: The Fourier Transformation

The time domain signal is not interpretable as it does not have the usual features of a spectrum of signal intensity *versus* frequencies or wavelengths. The NMR frequency domain (or as we shall see, the NMR spectrum with chemical shift information, Chap. 2) can be obtained using a Fourier transformation (FT). In this, the individual contributions of the different spins to the FID can be separated by means of applying FT to the time-dependent signal (which relies on the mathematical conclusion that any time-dependent function is equivalent to a frequency-dependent function) (Günther 1995; Wüthrich 1986; Derome 1987; Claridge 1999; Cavanagh et al. 1996; Keeler 2006; Evans 1996; Sanders and Hunter 1992). The mathematics and computation of the FT have been described in (Bracewell 1978). The FT will allow the splitting of the "clang" into the individual frequencies of each "bell" within the bell-ladder. In practice, the FT of the time-domain is achieved by using the Cooley-Tukey algorithm, which is reasonably fast even in computers with a moderate amount of available memory. The result of the FT is a complex function of frequencies in the sense that every point in the final spectrum has a real and an imaginary part. When this spectrum is stored onto a computer, the set of coefficients does not contain the final spectrum in the so-called *absorption mode* (all the peaks showing a maximum) and further processing is necessary (Chap. 3).

Several FIDs from simple spin systems and their corresponding transformed spectra are shown in Fig. 1.5. To illustrate, we consider the proton signal of the H_2O resonating at exactly the Larmor frequency (that is, the frequency of B_1 is

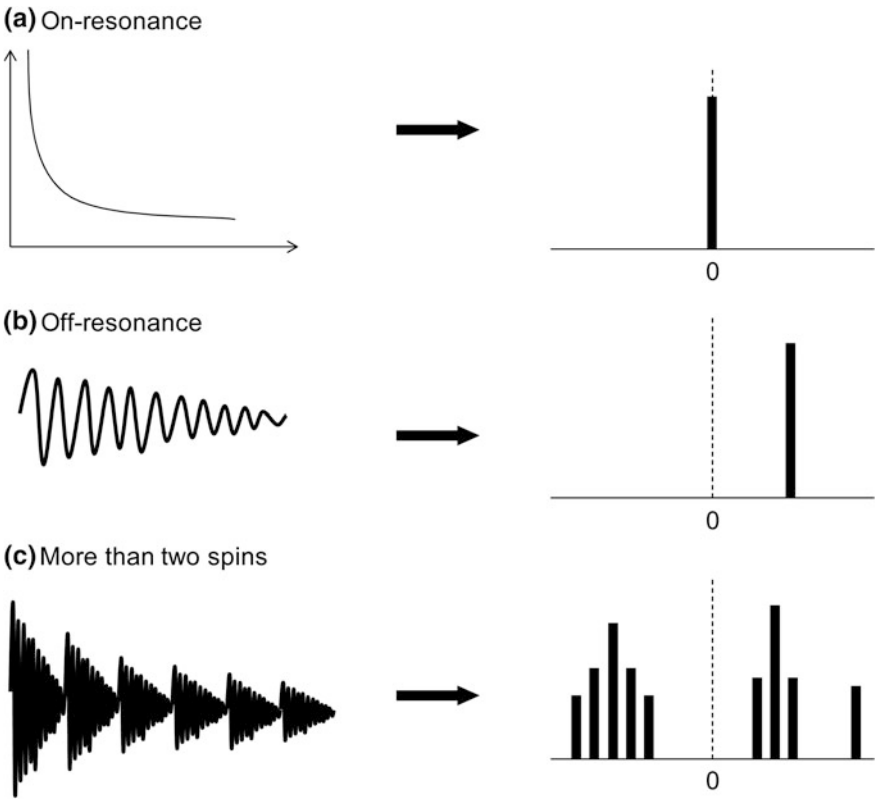

Fig. 1.5 FIDs and their spectra. **a** A simple FID (*left*) of a single on-resonance nucleus and the corresponding Fourier Transform (FT) spectrum (*right*, in bold). **b** FID and FT spectrum of a single spin system whose resonance frequency is not the same as that of the pulse B_1 (off-resonance nucleus). **c** FID of a system composed of several spins with different resonance frequencies and the schematic resulting FT spectrum

on-resonance). The spectrometer frequency is subtracted electronically from the observed signal prior to digitization, and as the detector is placed in the rotating frame, we obtain a simple exponential decay, where the time constant of the exponential is T_2 (Fig. 1.5a). In this case, the spectrum renders a single resonance at zero (0) Hz frequency. In a second situation, where the Larmor frequency of the nucleus is different to that of B_1 (that is, the frequency of B_1 is *off-resonance*), the FID has sinusoidal oscillations of constant frequency whose envelope is a decreasing exponential with time constant T_2. The resonance will appear slightly shifted from the spectrometer frequency (above or below 0 depending on the difference between the spectrometer frequency and the Larmor one of the nucleus) (Fig. 1.5b). If we have two or more spins with the same or different resonance frequencies, we shall have a signal which is the sum of the different components (Fig. 1.5c), and the difference between the frequency signals is the same as the

difference in absolute frequencies. Therefore, the above discussion on the aspect and the shape of the spectra suggests that the relative frequencies of each nucleus are detected, although the absolute frequencies of the observed nuclei are the same. This apparently arbitrary choice of the reference frequency does not cause any problem, as NMR frequencies are conveniently calibrated (Chap. 2). It is important to indicate that, prior to the FT, the acquired data can be manipulated to enhance its appearance or information content. We shall describe these "cosmetic" methods in Chap. 3.

1.4.2 Multipulse Experiments: Measurement of the T_1- and T_2-Relaxation Times as Examples

The above discussion is a simplification: modern NMR is not a single-pulse technique. The richness and power of modern NMR relies on the application of series of pulses between interleaved delays during which the magnetization of nuclear spins evolve. These pulses are applied in combinations with different lengths and phases (that is, along different axis), and to different nuclei at the same time or between the time delays. A series of pulses applied to extract required information from a molecule is called a *pulse sequence*. The idea of applying different pulses with different phase angles is of central importance in NMR; combining the collected data from sets of offsets of experiments in an appropriate manner allows removal of imperfections and selection of relevant signals in a process called *phase cycling*.

Here, we shall describe briefly two examples of pulse sequences, applied to a single type of nucleus. In Chaps. 3 and 4, we shall describe pulse sequences combining the magnetization of several nuclei. The sequence examples described here have been designed for the measurement of T_1 and T_2-relaxation times:

(a) *The inversion-recovery experiment*
The experiment consists on the application of two pulses: the first of 180° and the second, after a certain delay τ, of 90° applied both along the x-axis. Thus, the pulse sequence can be written as: $(180)_x$-time-$(90)_x$-acquisition (Fig. 1.6a). Initially, the magnetization M is aligned along the z-axis and the $(180)_x$ pulse inverts it into the –z-axis. With the application of the following $(90)_x$, we tilt the whole magnetization back on the xy-plane, to be precise on the y-axis. By varying the time between both pulses, we can study how long it takes for the magnetization along the z-axis to recover, and therefore measure T_1.

(b) *Spin-echo experiment*
The simplest sequence is $(90)_x$-time-$(180)_x$-time-acquisition, although several modifications have been described (Derome 1987; Claridge 1999) (Fig. 1.6b). After the initial $(90)_x$ that tilts M on the y-axis, the magnetization starts fanning out due to the different chemical environments of each nuclei and the intrinsic inhomogeneities of B_0. The application of a perfect $(180)_x$ takes the

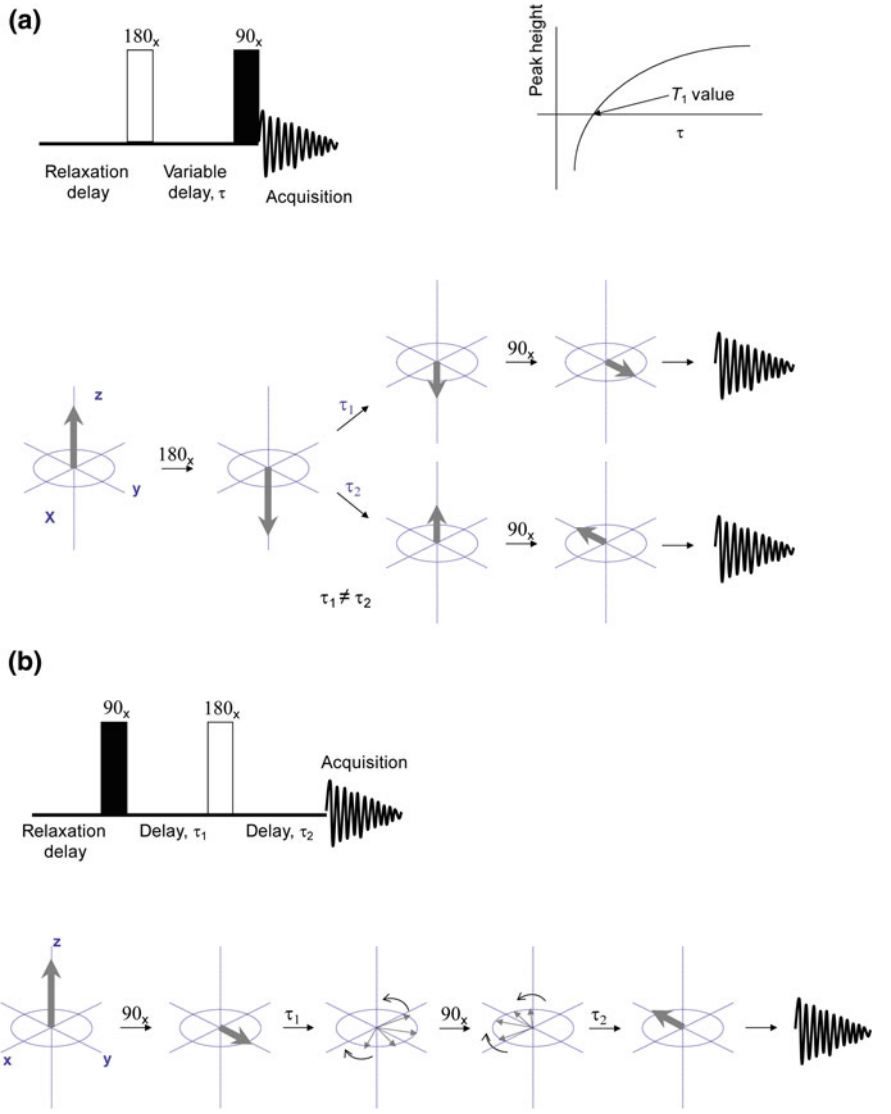

Fig. 1.6 Multi-pulse experiments to measure relaxation times. **a** Inversion-recovery pulse sequence represented with the vector model. *Top left* is the pulse sequence of the experiments (the 90° pulse is shown as filled rectangles and the 180° pulse is shown as *blank rectangles*). *Top right* is the graphical representation of peak intensity *versus* the variable delay τ, which yields T_1 at the intersection point with the x-axis. **b** The spin-echo sequence (Carr-Purcell). On the top, the pulse sequence is shown. On the *bottom*, the graphical representation of the behaviour of the spins according to the vector model is shown. The *arrows* indicate spins which are split due to the T_2-effects; the curved arrows around those spins indicate their circular movement

magnetization vectors on the other side of the xy-plane, and after a time-delay of the same duration as the one between pulses, the vectors will be aligned again along the −y-axis, where they will be detected. Varying the time (delay) between pulses will provide a measurement of T_2.

1.5 Practical Aspects of NMR

In this section, we describe some of the practical and instrumental aspects of high-resolution, solution-state NMR spectroscopy. We do not cover aspects such as performance-checking of the spectrometer, determination of its sensitivity or optimization of the signals line-shape, since those experimental aspects are already described in the manufacturer's instructions. Any reader interested in gaining a deeper knowledge on NMR practical aspects is referred to specialized books (Derome 1987; Claridge 1999; Berger and Braun 2003).

1.5.1 The Magnet

Figure. 1.7 shows a schematic overview of a modern NMR spectrometer where the static magnetic field is provided by superconducting materials. The sample is introduced within the magnet as indicated. We shall describe first how the magnet works and in Sect. 1.5.2 how the frequencies from the probe are handled.

The main solenoid producing the B_0 field is placed in a liquid helium bath (at a temperature of 4 K); under these conditions, the electrical resistance of the coil is essentially null. The helium container is surrounded by a liquid nitrogen Dewar

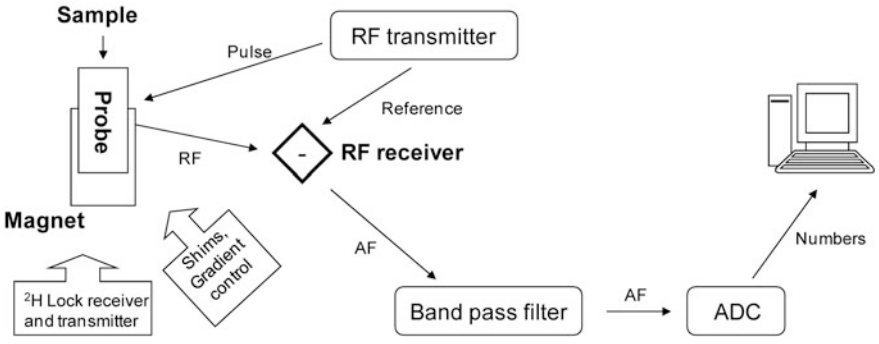

Fig. 1.7 Components of an NMR instrument. Schematic representation of a modern NMR instrument. The receiver reference frequency (RF) is subtracted to leave only audio frequencies (AF) which are digitised in the ADC

vessel (77 K) designed to reduce the loss of He (Fig. 1.8a). This second vessel is isolated from the exterior by a high vacuum chamber. Once the system is energized, the magnet operates indefinitely, free from any external power source. The basic maintenance requires periodical refilling of nitrogen (every 7–10 days) and of liquid helium (every 4–10 months depending on the magnet and the manufacturer). Additional cryo-coils are placed in the He-bath to partially correct any field inhomogeneity.

The magnet is vertically intersected by the room-temperature shim tube. This contraption houses a collection of electrical coils (controlled by software) known as *shim coils* (Sect. 1.5.4) that generate their own small magnetic fields (Fig. 1.8). The shims are used to trim the B_0 and to eliminate residual inhomogeneities of the field. The adjustment of these electrical coils is specific to each sample. The actual NMR sample is contained within a cylindrical glass tube inserted into a plastic or ceramic spinner which is introduced into the magnet from the top of the shim tube using a flow of compressed air or N_2 that drops the tube and spinner into the probe-head (Fig. 1.8b). The sample is in solution and its volume and final concentration depends on the particular application (Günther 1995; Derome 1987; Claridge 1999). For some NMR experiments and low fields (200–300 MHz), the sample is spun at 10–20 Hz to average to zero the field inhomogeneities in the xy-plane, improving signal resolution. However, the spinning introduces additional signal modulations known as *spinning sidebands*, and it is not normally applied at higher fields. At the exact centre of the magnetic field sits the head of the probe, the heart of the NMR spectrometer where the cylindrical tube containing the sample is placed.

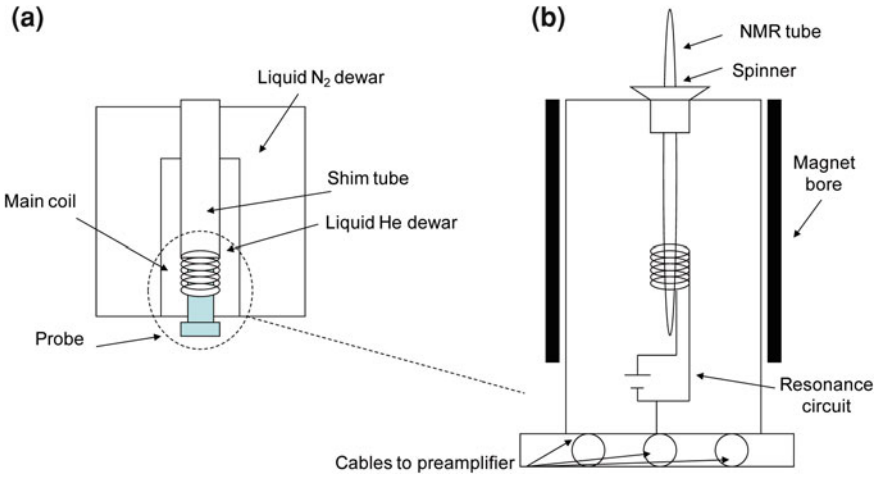

Fig. 1.8 Components of the magnet. **a** Schematic representation of the magnet, showing the He and N_2 chambers, the main coils and the probe-head. **b** Schematic view of the bore with the sample tube, within the spinner, placed in the probe-head. The cables of the preamplifier are also routed to the wobble-unit

1.5.2 The Probe

The NMR probe has two key functions. First, it is the means by which the radiofrequency power is transmitted to the sample for the perturbation of the spin system populations (that is, it creates the pulse). And second, it is required to detect the electromotive force generated by the rotating bulk magnetization, which is in the order of 10^{-9}–10^{-5} V (at the lower end, these values are similar to the amplitude of the electronic noise introduced by the coil). Therefore, the probe houses both the transmitter and receiver coils of the electromagnetic radiation (in modern NMR probes the same coil acts as transmitter and receiver) and associated circuitry, such as the optional gradient coils (Sect. 1.5.6). Probes can be manufactured in various sizes depending on the diameter of the sample tube that it fits around, with the most common being 5 mm, although other sizes are available (e.g. 3, 8 or 10 mm).

Most probes contain two coils: an inner coil tuned to deuterium (the *lock*, Sect. 1.5.3) and a second frequency, whereas the outer coil is tuned to a third and sometimes a fourth frequency. The deuterium channel is placed on the inner coil on most probes as the proximity to the sample increases the sensitivity and renders shorter pulse-lengths. For probes designed to detect ^{1}H (the so-called *inverse probes*) the proton is the second frequency on which the inner coil is tuned. For probes not designed for ^{1}H detection, the second nucleus the inner coil is tuned to can vary.

The receiver coil is at the centre of the magnetic field and the sample in the NMR tube is completely surrounded by this coil. The resonance circuitry inside the probe also contains capacitors that require tuning every time the sample is changed. The probe is connected to a preamplifier, which performs an initial amplification of the NMR signal. The preamplifier contains a wobbling unit required for tuning and matching the probe for each sample. In the wobbling unit the frequency is continuously swept back and forth through the resonance of the nucleus to be observed, covering a bandwidth of 4–20 Hz. A large influence on the tuning and matching of the probe is the dielectric constant of each individual sample, which affects the dielectric constant in the inner coil region and therefore its impedance; high ionic strength (high salt concentration) will significantly increase the length of the pulses.

The amplifiers are low-noise audio-amplifiers which boost the amplitude of the incoming signal to yield a larger undistorted one. In addition, current NMR spectrometers use amplifiers to convert the radiofrequency (RF) to audio-frequencies (AF), by carrying out the subtraction of the reference frequency from the detected signal (Sect. 1.4), which are easier to handle (Fig. 1.7). An ideal amplifier would be a wire with a high-gain, located adjacent to the probe to reduce signal losses due to the connecting cables. The signal is converted from analogue to digital by an analogue-to-digital converter (ADC or digitizer). It is necessary to use an ADC because the signal from the probe is recorded in analogue form (since the FID is the superposition of various frequencies), but it must be in a digital form

to apply the FT in the computer. The output signal of the amplifier must match the dynamic range of the ADC. To faithfully reproduce the analogue signal, the sampling rate of the ADC must be at least twice the frequency of the signal (*Nyquist condition*). Even if the Nyquist condition is fulfilled, the ADC makes an approximation to the true signal, since it represents the superposition of the frequencies by 16 to 18 bits (that is, the most intense signal can be digitized as 2^{18}). This can have serious consequences for the dynamic range (the limits on weak and strong signals we can observe): for instance, signals with less than $1/2^{18}$ of the signal amplitude cannot be distinguished. Errors in the digitization of strong signals can originate "noise" on the baseline, which may "swamp" weak signals. Therefore, the receiver gain (the amplification of the signal) should be adjusted in such a way that the most intense signal completely fills the range of the amplifier.

1.5.3 The Lock-System

The frequencies generated in modern NMR spectrometers are very stable, but the Larmor frequencies ($\omega_0 = \gamma B_0$) of the nuclei are not. Since there is no inherent instability in the constant gyromagnetic ratio (γ) of the nuclei, the variability must come from the static magnetic field B_0. The field created by the superconducting magnet decays slowly with time and it is not stable enough for high-resolution NMR. To improve the stability of the field, an electronic device has been incorporated into modern NMR spectrometers tasked with the acquisition of a second NMR experiment in a continuous and automatic manner. This experiment uses deuterium (^{2}H) as the monitored nucleus, which is why the inner coils of the probes are always tuned to this nucleus. To ensure the presence of the ^{2}H isotope in reasonable amounts in the sample, 5–10 % of ^2H_2O is added to aqueous samples or fully deuterated organic solvents, like $CDCl_3$ or DMSO-d_6, are used.

This second, stabilising experiment consists of a continuous train of pulses applied to the sample at the Larmor frequency of deuterium, which will vary depending on the solvent used. The Larmor frequency of the deuterons is established by bringing the signal onto resonance through the manual adjustment of the field. The electronic circuit of the device maintains the on-resonance condition, locking the field to the exciting frequency of deuterium; however, since all frequencies in modern spectrometers are generated from the same source, all the excitation frequencies for any nuclei explored in the experiment are locked. The system works by using a feedback loop, which generates corrections to the B_0, such that the on-resonance frequency of the deuterium in the solvent remains constant.

1.5.4 The Transmitter/Receiver System: Quadrature Detection

We know from trigonometry that the values of cos(α) and cos(–α) are equal. Therefore, since we are registering the decay of the transverse magnetization after a radiofrequency pulse with a single receiver coil located along one of the axis in the xy-plane (Fig. 1.9a), we cannot distinguish between frequencies rotating slower or faster than the frequency of reference (*carrier frequency*), that is, negative or positive frequencies, respectively.

One possible solution would consist in setting up the carrier frequency on one side of the spectrum instead of the centre, but this would increase the noise in the spectrum, which would be only averaged on "one" side of the reference frequency. Another solution to distinguish the positive from the negative frequencies would be to arrange a second detector along the other axis (the x-axis in our discussion, which is shifted 90° with respect to the y-axis); then, by collecting the sine projection of the transverse magnetization it will be possible to differentiate

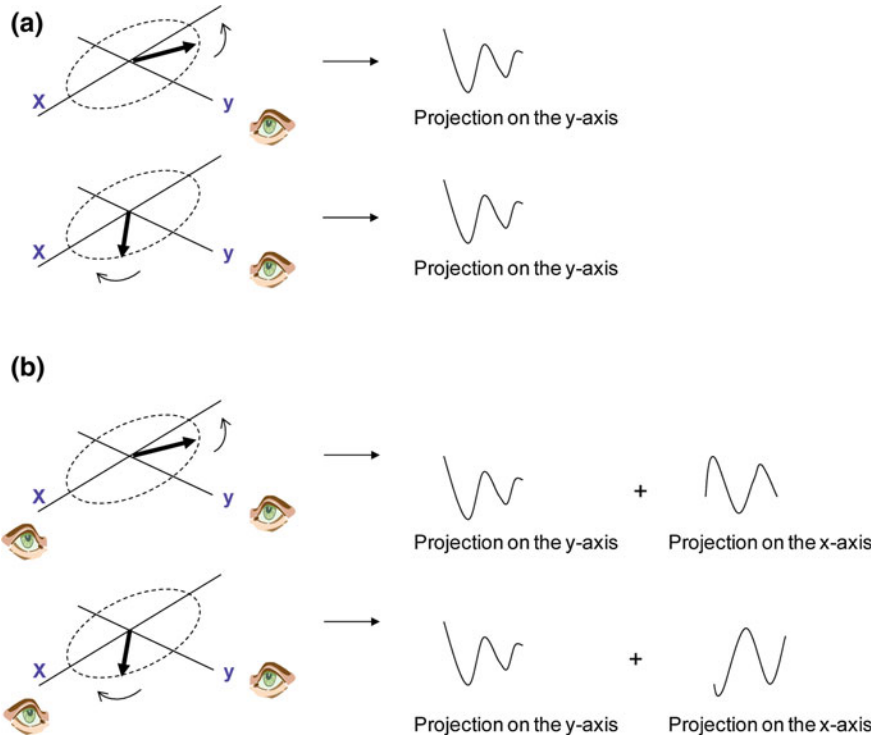

Fig. 1.9 The quadrature detector. **a** A single detector cannot distinguish between positive and negative frequencies. **b** Two detectors located in quadrature (that is, they are shifted by 90°) can discriminate between the sense of precession of two signals

the sign of the frequencies (Fig. 1.9b). This approach is known as *quadrature detection* since both detectors are shifted by a quadrant (90°) of a circle. However, in a cramped system like an NMR probe, the introduction of a second coil is difficult. Therefore, the sine- and cosine-modulated components of the signal come from a different trick: the signal coming from the receiver coil is divided into two signals by a splitter. Both parts are mixed with the transmitter frequency (the carrier frequency). The phase of the transmitter frequency that is added to one of the split signals differs by 90° from that of the other half, and therefore, we shall have the equivalent of having two detectors. Experimentally, sine and cosine-modulated signals are sometimes amplified slightly different, and artefacts called *quadrature images* can appear. These artefacts can be recognized because they are "mirrored" about the zero frequency (the middle of spectrum, where the carrier frequency is located). To avoid these undesired effects, modern spectrometers utilize oversampling, where a larger spectral width is used such that the quadrature images do not fall into the observed spectrum.

1.5.5 The Shim System

Present generation magnets have field inhomogeneities of 1 part in 10^9, thanks mainly to the careful design of the internal solenoid, although it can still be considered an insufficient value for the acquisition of high resolution NMR experiments. The shim system consists in a hardware device that corrects for slight differences in the local magnetic fields. It is constituted of two parts: the cryo-shim system and the room-temperature shims. The principle behind both is alike: small coils are supplied with highly regulated electrical currents. These currents produce small magnetic fields that correct the field inhomogeneities created by the main solenoid. There are several of those coils positioned at diverse geometries to produce field corrections with different orientations. The cryo-shim system is located inside the He bath and after the initial adjustment by the engineers during the start-up of the instrument, no further manipulation is required. The room-temperature shim system is set coaxially in the bore of the magnet, it is user-controlled and needs adjusting every time a new sample is placed in the instrument. The room-temperature systems (of which there are typically 20 to 30 on a modern instrument) are usually grouped into two classes: the on-axis spinning systems (z, z^2, z^3, z^4) and the off-axis non-spinning shims (x, y, xy, and others). The *on-axis* shims only correct for field inhomogeneities along the z-axis, being highly dependent on the solvent and the height to which the NMR tube is filled. The *off-axis* shims normally do not have to be extensively adjusted, and only x, y, xz and yz need some tinkering with for every new sample. In general, shimming is only practiced on a small fraction of the total available number of shims. Shimming improvement is usually performed by either observing the intensity of the lock signal (which one aims to maximize in height) or by monitoring the shape

of the FID. However, the recent introduction of the automation of the process of shimming has eased this pre-acquisition step considerably.

1.5.6 Pulse Field Gradients

One of the most important technical advances in high-resolution NMR during the last decade of the twentieth century was the introduction of *pulse field gradients* (PFG), or *gradients* for short. In general, gradients are used to diffuse unwanted signals and thereby sharpen the desired ones (see below). Gradients had been applied in magnetic resonance imaging for a long time, but their application to high-resolution NMR was limited by technical problems (Hurd 1990). Among these difficulties was the production of *eddy-currents* generated during the application of the gradient pulse. These are currents generated in the components that surround the sample, like the circuitry and the shims themselves, which in turn generate magnetic fields within the sample. Since these currents can last for hundreds of milliseconds, acquisition of high-resolution spectra was hampered under their influence. The most effective way to suppress the generation of *eddy-currents* (and therefore, the solution to the technical problem) is the use of actively-shielded gradient coils, currently used in all commercially available gradient probes. This extra gradient coil generates a second field outside the active sample region, opposing and cancelling out the field produced by the inner coil. In the next paragraph, we shall describe the physical basis of gradients and how they are produced. Any reader interested in the more theoretical aspects and applications of pulse field gradients can find a more detailed description in recent literature (Keeler et al. 1994).

1.5.6.1 Gradients

If we imagine the NMR sample as divided into small disks, after a radiofrequency pulse each disk will have a magnetization vector in the transversal xy-plane, but each of them will experience a slightly different local magnetic field according to its position in the sample (Fig. 1.10, left). If a linear variation of a magnetic field is imposed for a short time (a gradient pulse) along the z-axis (grey short arrows), chemically equivalent spins will experience different fields according to their position along the z-axis, and therefore they will precess with diverse frequencies and rotate at dissimilar angles. If the gradient is long and powerful enough, the sum of all transverse magnetizations will be null and there will be no detectable NMR signal (since the signal is highly inhomogeneous). The gradient will have completely defocused the magnetization. However, although the magnetization is globally null it is still present in the sample, and the application of a second gradient (with the appropriate power, length and phase) will undo the dephasing achieved with the first gradient yielding a refocusing of all phases in the imaginary

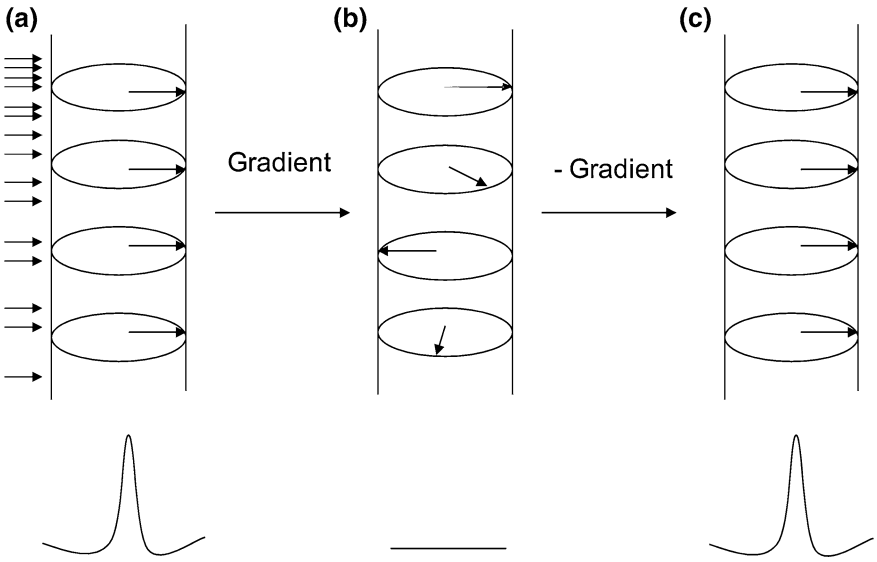

Fig. 1.10 How PFGs work. **a** In a homogenous magnetic field, chemically identical spins have the same phase and Larmor frequency after the application of a (90°)-pulse, yielding a single sharp resonance (*bottom*). The *grey arrows* on the *left side* indicate the field variation, that is, the gradient (with smaller intensity at the *bottom* of the figure and higher at the top). **b** After the application of a linear gradient, the spins have adopted different phases and no signal is detected. **c** Application of a second identical gradient with the opposite direction refocuses the individual spins resulting in a re-phased peak

sample disks, resulting in observable transversal magnetization (Fig. 1.10, right). The concept of defocusing the signals and refocusing only the desired ones (by modulating the power, the length and the phase of the refocusing gradient) has made PFGs extremely useful in NMR. In fact, conversely to what happens with radiofrequency pulses, accurate strength and pulse calibration of PFGs are not required for experimental success, provided that the PFG is strong enough to dephase unwanted magnetization. However, it is important to ensure that the PFGs are reproducible and that the gradient ratios of the pulse gradients used to defocus and refocus are kept constant.

Gradients are used in high-resolution NMR in three general applications. First, the removing of unwanted magnetization such as the solvent signal, which is of widespread use in aqueous biomolecular samples. PFGs also eliminate responses resulting from imperfections of pulse sequences, an important application that replaces the use of time consuming phase cycles (Sect. 1.4.2). Second, PFGs are used to select magnetization routes crucial to the NMR experiment while discarding non-relevant ones. We shall not describe this application, which is beyond the scope of this book [the interested reader can find more information in (Claridge 1999; Cavanagh et al. 1996; Keeler et al. 1994)]. And finally, gradients are used in shimming (Vanzijl et al. 1994; Barjat et al. 1997), where inhomogeneities of the

magnet due to the sample are encoded in the applied gradients (as phase differences, Fig. 1.10) and used to correct them.

Regarding gradient generation, they can be produced by offsetting one of the shim currents from its optimum value (for instance, driving the z-shim at its maximum current), although such set-up only creates weak fields and offers no control over the gradient amplitude. In current probes, there are dedicated-gradient coils surrounding the usual radiofrequency solenoids, together with an appropriate gradient amplifier and a second shield-gradient coil (Sect. 1.5.2). The field gradient is generated by applying a current to the gradient coils (the typical highest value is 0.5 Tm^{-1} or 50 Gcm^{-1}) or by reversing it, if an inversion of the gradient phase is sought.

Finally, the use of gradients might appear incompatible with locking the field, since gradients introduce inhomogeneities which would preclude the electronics from keeping the ^{2}H lock signal fixed. However, the corrections introduced by the lock are the result of long-time monitoring periods of the static field, while the perturbations caused by gradients only last a few milliseconds at most. In experiments with gradient application, the lock should be highly "damped" (in a sense, disconnected) to avoid the computer trying to correct the field each time is recovering from the effect of an applied gradient.

1.5.7 Sample Preparation

Most NMR experiments in the biology/biochemistry field are carried out in H_2O, with the addition of 5–10 % of $^{2}H_2O$ for the lock signal. In some cases, especially when working with peptides or protein fragments, organic solvents such as trifluoroethanol or dimethyl sulfoxide are used. For experiments with proteins associated with lipid membranes, the use of detergents such as sodium dodecyl sulphate (SDS) is required, and in some cases, conventional high-resolution NMR methods cannot be used; an alternative to gain structural insight into those systems is offered by special techniques like solid-state NMR. Organic solvents are usually employed in chemistry, most of them commercially available in deuterated forms to allow acquisition of ^{1}H-NMR spectra without interference from the solvent signal.

As NMR is an intrinsically insensitive spectroscopic technique, experiments aimed at structural molecular elucidation tend to be performed at high sample concentrations (in the mM–M range). Therefore, the molecule must be soluble at those concentrations (i.e. monodisperse), and be stable enough to last during the usually long acquisition times. In the case of stable biomolecules, NMR experiments are normally acquired at pH $\leq$ 7.0, since under these conditions the hydrogen-exchange reaction of amide protons with water is minimised. Buffer components presenting active spins that could obscure any of the resonances of the sample are to be avoided, although deuterated chemicals can be employed in homonuclear ^{1}H-detected experiments. There is no need for the use of deuterated solvents for the acquisition of NMR experiments observing other nuclei rather than ^{1}H (e.g. ^{13}C, ^{15}N). High ionic-strength samples decrease the signal-to-noise ratio

(S/N) as the presence of local magnetic fields caused by the ions produce an increase in pulse lengths. Finally, as the resonance line width decreases (and therefore, resolution increases) with temperature, NMR experiments are normally acquired at room temperature or higher, provided that the molecule does not suffer any conformational changes or degradation. If a system under study requires low temperatures, NMR experiments can be carried out even below 173 K by keeping the sample cold with a continuous flow of liquid N_2 and using organic solvents with low freezing points (CH_2Cl_2, tetrahydrofuran (THF) or others).

References

Barjat H, Chilvers PB, Fetler BK, Horne TJ, Morris GA (1997) A practical method for automated shimming with normal spectrometer hardware. J Magn Reson 125:197–201

Berger S, Braun S (2003) 200 and more NMR experiments. Wiley-VCH, New York

Bracewell RM (1978) The Fourier transform and its applications, 2nd edn. McGraw Hill, New York

Cavanagh J, Fairbrother WJ, Palmer AG 3rd, Skelton NJ (1996) Protein NMR spectroscopy. Principles and practice, 1st edn. Academic Press, New York

Claridge TDW (1999) High-resolution NMR techniques in organic chemistry. Pergamon Press, Oxford

Derome AE (1987) Modern NMR techniques for chemistry research. Pergamon Press, Oxford

Ernst RR, Bodenhausen G, Wokau A (1987) Principles of NMR in one or two dimensions. Clarendon Press, Oxford

Evans JNS (1996) Biomolecular NMR spectroscopy. Oxford University Press, Oxford

Farrar TC, Becker ED (1971) Pulse and Fourier transform NMR. Academic Press, New York

Günther H (1995) NMR spectroscopy: basic principles, concepts and applications in chemistry, 2nd edn. Wiley, Chichester

Harris RK, Mann BE (1978) NMR and the periodic table. Academic Press, London

Hurd RE (1990) Gradient enhanced spectroscopy. J Magn Reson 87:422–428

Keeler J (2006) Understanding NMR spectroscopy, 2nd edn. Wiley, Chichester

Keeler J, Clowes RT, Davis AL, Laue ED (1994) Pulse-field gradients: theory and practice. Methods Enzymol 239:145–207

Mason J (1987) Multinuclear NMR. Plenum, New York

Sanders JKM, Hunter BK (1992) Modern NMR spectroscopy, 2nd edn. Oxford University Press, Oxford

Vanzijl PCM, Sukumar S, Johnson MO, Webb P, Hurd RE (1994) Optimized shimming for high resolution NMR using three-dimensional image-based field mapping. J Magn Reson 111:203–207

Wüthrich K (1986) NMR of proteins and nucleic acids. Wiley, New York